Further study of the Mn^{2+} EPR centre in ferro- and para-elastic $BiVO_4$:spin Hamiltonian parameters and temperature dependence

1992 J. Phys.: Condens. Matter 4 587

(http://iopscience.iop.org/0953-8984/4/2/027)

J. Phys.: Condens. Matter 4 (1992) 587–598. Printed in the UK

Further study of the Mn^{2+} EPR centre in ferro- and para-elastic $BiVO_4$: spin Hamiltonian parameters and temperature dependence

T H Yeom†, S H Choh† and M S Jang‡

† Department of Physics, Korea University, Seoul 136-701, Korea
‡ Department of Physics, Pusan National University, Pusan 609-735, Korea

Received 20 August 1991

Abstract. The electron paramagnetic resonance (EPR) of an Mn^{2+} ($S = 5/2$) impurity in the ferroelastic and para-elastic phase of $BiVO_4$ crystals with a single domain, grown by the Czochralski method, has been investigated using an X-band spectrometer. The rotation patterns of the resonance fields measured on the crystallographic planes are analysed: $g = 1.9940 \pm 0.0009$, $D/h = 2.443 \pm 0.002$, $E/h = 0.4912 \pm 0.0009$, $F/h = 0.094 \pm 0.002$, $B_4^2/h = 0.0$, $A_x/h = 0.27 \pm 0.02$, $A_y/h = 0.25 \pm 0.02$, and $A_z/h = 0.33 \pm 0.02$ GHz at room temperature ($< T_c = 528$ K); and $g = 1.994 \pm 0.001$, $D/h = 0.000 \pm 0.004$, $E/h = 0.000 \pm 0.004$, $F/h = 0.00 \pm 0.01$, $A/h = 0.25 \pm 0.01$ GHz at $T = 535$ K ($> T_c$). The principal x, y, and z axes of the D-tensor are found to be along the crystallographic $\bar{b}$, $c + 45°$ and $\bar{a} + 45°$ axes, respectively. This Mn^{2+} centre has the correct principal axes system of the D-tensor compared with the previous Mn_I centre. The D-value decreases as the temperature increases in the range 107–535 K. It is proposed that the Mn^{2+} ion substitutes for Bi^{3+} without nearby charge compensation.

1. Introduction

Bismuth vanadate ($BiVO_4$), first synthesized in 1963 (Roth and Waring), was found to be ferroelastic (Bierlein and Sleight 1975). Recently, there have been a great number of experiments, such as x-ray and powder neutron diffraction (David *et al* 1979), Raman scattering (Pinczuk *et al* 1977, 1979) and NMR (Lim *et al* 1989), to investigate its structural changes, phase transitions and optical properties. The structure of the domains has been investigated by the ^{51}V NMR and x-ray diffraction techniques (Choh *et al* 1985, Moon *et al* 1987).

An EPR study of Gd^{3+}, Er^{3+} and Mn^{2+} in $BiVO_4$ single crystals has also been reported (Baran *et al* 1985). The angular dependences of the EPR spectra of these ions were studied in the temperature range 4.2–650 K, and domains with an angle of 90° were proposed from the EPR spectra. It was suggested that Gd^{3+}, Er^{3+} and Mn^{2+} replace Bi^{3+}, Bi^{3+} or V^{5+}, and Bi^{3+}, respectively, and that there are two types of centres for Mn^{2+}: one without any accompanying defect (Mn_I) and the other with a vacancy in the immediate environment (Mn_{II}).

In our preceding papers, the phase transition and domain structure have been studied mainly by the NMR of ^{51}V (Choh *et al* 1985, Moon *et al* 1987, Lim *et al* 1989). The present work is an extension to include EPR of the paramagnetic impurity

0953-8984/92/020587+12$03.50

in $BiVO_4$ because EPR is a sensitive technique for distinguishing domain structures (Baran *et al* 1985). Meanwhile, we have observed an Mn^{2+} EPR centre in the ferroelastic and para-elastic phases of $BiVO_4$ single crystals with a single domain. In this paper, the relationship between the principal axes of the zero-field splitting tensor and crystallographic axes is examined by means of the rotation patterns of the EPR spectra and is discussed in terms of the defect structure. The temperature dependence of the zero-field splitting parameters and the ferroelastic phase transition are discussed in terms of the EPR spectra measured in the range 107–535 K. This Mn^{2+} centre is different in its principal axes system of the D-tensor from the Mn_I centre reported by Baran *et al* (1985). This preliminary result was given at a Korean Physical Society Meeting (Yeom *et al* 1990).

2. Crystal structure

Bismuth vanadate crystal undergoes a reversible second-order phase transition at about 528 K ($= T_c$) between the monoclinic fergusonite and the tetragonal scheelite structure (Dudnik *et al* 1979). The ferroelastic phase of $BiVO_4$ has the point group $2/m$ with the unit cell dimensions $a = 5.1966$ Å, $b = 11.704$ Å, and $c = 5.0921$ Å, and $\beta = 90.38°$ at room temperature. In the para-elastic phase the space group is $4/m$ with the lattice parameters $a = c = 5.1507$ Å, $b = 11.730$ Å, and $\beta = 90.0°$ at 573 K (David *et al* 1979). The para-elastic tetragonal structure of $BiVO_4$ is shown in figure 1, where the arrows mark the displacements of the ions below T_c.

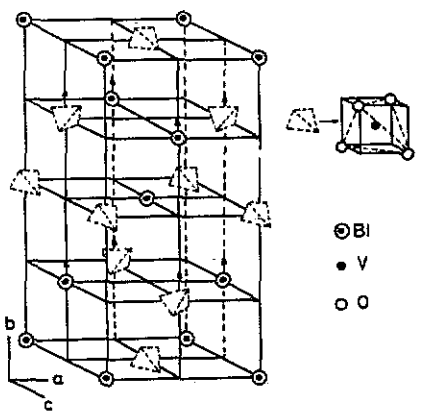

Figure 1. The para-elastic tetragonal structure of a $BiVO_4$ single crystal. The arrows show distortion from the para-elastic to the ferroelastic structure.

The displacements of Bi^{3+} and V^{5+} are along the b axis: both cations move in the same direction (Sleight *et al* 1979). The displacements of the Bi^{3+} ions play a major role in the transition (Wood and Glazer 1980). In the ferroelastic phase, the vanadium atom with different bond lengths ($V–O_I$ and $V–O_{II}$) is located in a distorted oxygen tetrahedron, and the bismuth atom is coordinated by eight distorted VO_4 tetrahedra. $BiVO_4$ single crystals grown by the Czochralski method have either single or twin domain structures (Moon *et al* 1987).

3. Experimental procedure

A sample crystal with a single domain, confirmed by x-ray diffraction and ^{51}V NMR, was selected for the EPR study. The manganese was not deliberately doped into the crystal but was contained in the starting material as an impurity. The concentration of the Mn impurity in the crystal was not chemically analysed; however, it is estimated to be less than 0.01 wt%. The crystallographic principal axes of the specimen were determined by the x-ray Laue method.

The rotation patterns of the resonance fields on the crystallographic *ab*-, *bc*- and *ca*-planes were obtained at 1° or 2° intervals at room temperature. On the other hand the temperature dependence of the EPR spectra was measured at three angles on the *ca*-plane including the z axis of the D-tensor. The rotation pattern of the resonance fields on the crystallographic *ca*-plane which contains the principal z axis of D-tensor was also obtained at 535 K ($> T_c$).

The equipment used for the EPR measurements was a Bruker X-band EPR spectrometer (ESP 300 series) with a TE_{102} rectangular cavity. The microwave frequency was kept in the range 9.800 ± 0.003 GHz (at room temperature) and 9.531 ± 0.003 GHz (at 535 K), respectively, during the measurements, and the microwave frequency counter was calibrated by observing the DPPH signal. An NMR gaussmeter was used for measuring the resonance magnetic fields. From the experimental data for the three crystallographic planes, the accuracy of the sample alignment is estimated to be within $\pm 1.0°$.

4. Experimental data

A typical EPR spectrum measured at room temperature is shown in figure 2, where we deal with only the spectrum of the Mn^{2+} ion. The five groups of lines labelled 1, 2, 3, 4 and 5 are the fine structure of Mn^{2+} ($S = 5/2$), and the six lines within each group are the hyperfine structure of ^{55}Mn ($I = 5/2$, 100% abundance).

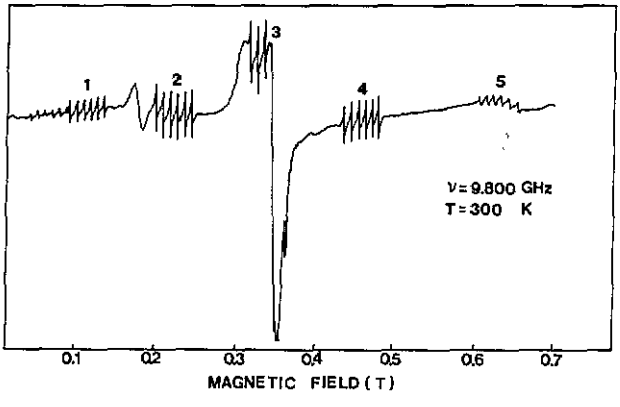

Figure 2. EPR spectra of Mn^{2+} and other impurities in a $BiVO_4$ single crystal. The magnetic field was applied along the bisector of the c and $\bar{a}$ axes in the *ca*-plane.

The rotation patterns of the resonance fields of Mn^{2+} in $BiVO_4$ on the crystallographic *ab*-, *bc*- and *ca*-planes are shown in figures 3, 4 and 5, respectively. The

experimental points taken at the centre of each fine structure are indicated by open circles, and the calculations to be discussed later are indicated by full curves. The reason we have fewer experimental points in figures 3 and 4 than in figure 5 is the fact that the signal intensity is strongly dependent on the direction of the applied magnetic field and the hyperfine spectra mingle with each other when the resonance fields approach nearer. This dependence is found to be associated with the Zeeman interaction and the principal axes system of the zero-field splitting (see figure 7).

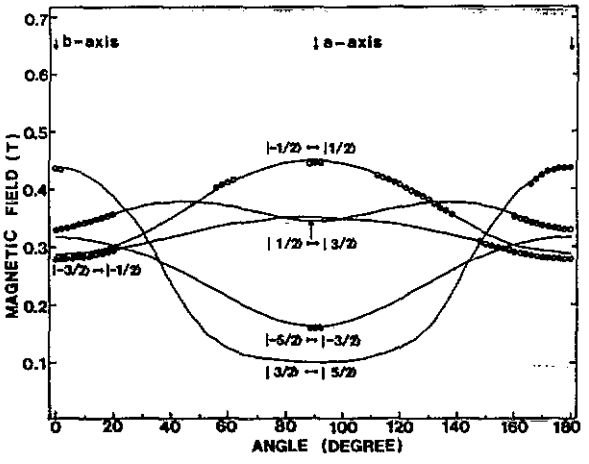

Figure 3. Rotation pattern for the Mn^{2+} resonance in the ab-plane of $BiVO_4$.

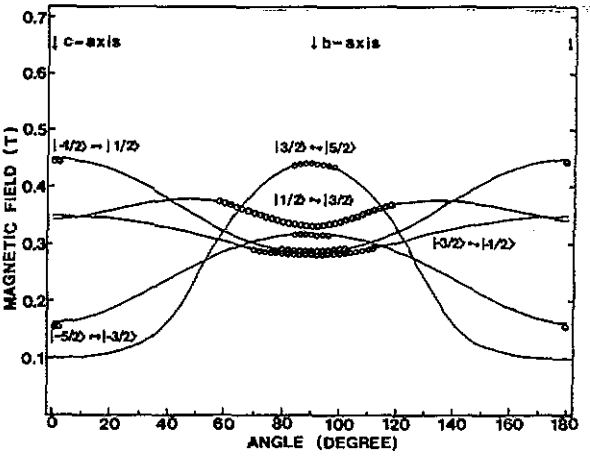

Figure 4. Rotation pattern for the Mn^{2+} resonance in the bc-plane of $BiVO_4$.

The data points in these figures show symmetric angular dependences. One principal axis of the zero-field splitting tensor automatically turns out to be along the b axis for which the rotation patterns are symmetric on the ab- and bc-planes. Consequently, the remaining two principal axes are on the ca-plane, perpendicular to the b axis. Accordingly, from the angular dependence of the resonance fields on the ca-plane in figure 5, the two other principal axes of the zero-field splitting tensor are determined

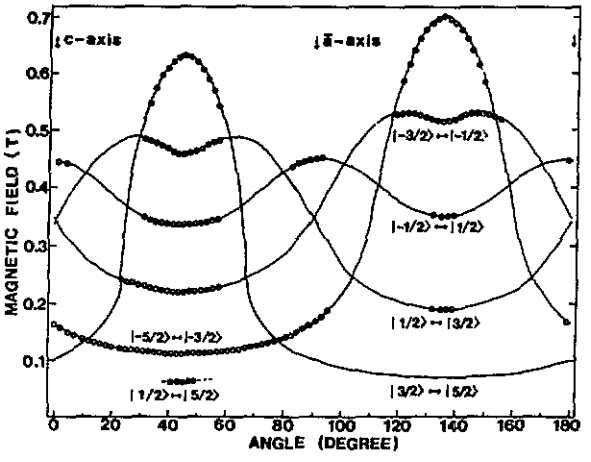

Figure 5. Rotation pattern for the Mn^{2+} resonance in the ca-plane of $BiVO_4$.

to be $c + 45°$ (i.e. $\bar{a} - 45°$) and $\bar{a} + 45°$ (i.e. $c + 135°$), respectively. Actually the a, b, and c axes of ferroelastic $BiVO_4$ are not perfectly orthogonal (monoclinic); however, they may be approximated as orthorhombic (see the analysis).

To examine the temperature dependence of the EPR parameters for the Mn^{2+} impurity in a $BiVO_4$ single crystal, the resonance spectra were measured at thirteen different temperatures in the range 107–535 K. Among the three specific angles only the resonance field data with the magnetic field applied along the z axis of the D-tensor are shown in figure 6 for the three transitions: $|-\frac{1}{2}\rangle \leftrightarrow |\frac{1}{2}\rangle$; $|-\frac{3}{2}\rangle \leftrightarrow |-\frac{1}{2}\rangle$; and $|-\frac{5}{2}\rangle \leftrightarrow |-\frac{3}{2}\rangle$ as a function of temperature. The rotation pattern of the resonance fields of the Mn^{2+} ion in the para-elastic phase, showing no angular dependence, was also obtained. The five fine structure lines which consisted of six lines each, recorded at room temperature (e.g. figure 2), degenerated into only one with the six-line hyperfine structure in the para-elastic phase.

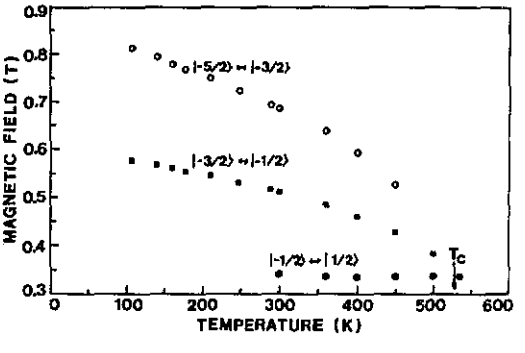

Figure 6. Temperature dependence of EPR spectra of Mn^{2+} in a $BiVO_4$ single crystal. Only three lines out of five are shown.

5. Analysis

The Mn^{2+} ion has the electron configuration $1s^2 2s^2 2p^6 3s^2 3p^6 3d^5$ and is an S-state ion

with $S = 5/2$ and a basic level of $^6S_{5/2}$. When this ion is embedded in a crystal, it experiences an intense crystal field produced by the neighbouring ions because the 3d shell of the Mn^{2+} ion is the outermost one. Consequently, fine structure arises from the crystal field and the spin–spin interactions, and the hyperfine structure results from the interaction between the nuclear spin of ^{55}Mn ($I = 5/2$, 100%) and its electronic spin. Accordingly, the experimental results for the resonance fields can be analysed with the usual spin Hamiltonian

$$H = H_Z + H_{zfs} + H_h \tag{1}$$

where the terms on the right-hand side are the Zeeman interaction, the fine structure (zero-field splitting), and the hyperfine interaction, respectively. The Zeeman term is

$$H_Z = \beta \boldsymbol{B} \cdot \mathbf{g} \cdot \boldsymbol{S} \tag{2}$$

where β is the Bohr magneton, $\boldsymbol{B}$ is the external magnetic field vector, $\mathbf{g}$ is the spectroscopic splitting tensor, and $\boldsymbol{S}$ is the effective electronic spin vector. The zero-field splitting term is

$$H_{zfs} = \sum_{kq} B_k^q O_k^q = \sum_{kq} f_k b_k^q O_k^q \tag{3}$$

where we have adopted the extended Stevens operators (O_k^q, $q < 0$ included) defined in Rudowicz (1985) as the reference notation. The second form (Bleaney *et al* 1954) was introduced for numerical convenience. The consistent convention (Altshuler and Kozyrev 1974, Newman and Urban 1975) for the 'scaled' parameters b_k^q, which prevails in recent literature, requires that $f_k = \frac{1}{3}$, $\frac{1}{60}$ and $\frac{1}{1260}$ for $k = 2$, 4 and 6, respectively. The general zero-field splitting term for the monoclinic structure (Rudowicz 1986) is

$$\begin{aligned} H_{zfs} = {} & B_2^0 O_2^0 + B_2^2 O_2^2 + B_4^0 O_4^0 + B_4^2 O_4^2 + B_4^4 O_4^4 + B_6^0 O_6^0 + B_6^2 O_6^2 + B_6^4 O_6^4 + B_6^6 O_6^6 \\ & + B_2^{-2} O_2^{-2} + B_4^{-2} O_4^{-2} + B_4^{-4} O_4^{-4} + B_6^{-2} O_6^{-2} + B_6^{-4} O_6^{-4} + B_6^{-6} O_6^{-6}. \end{aligned} \tag{4}$$

Although the ferroelastic $BiVO_4$ crystal is monoclinic, it may be considered orthorhombic because $\beta(90.38°)$ is nearly 90.0°, and the accuracy of our sample alignment is ±1.0°. The zero-field splitting Hamiltonian for orthorhombic symmetry is (Rudowicz 1985)

$$H_{zfs} = B_2^0 O_2^0 + B_2^2 O_2^2 + B_4^0 O_4^0 + B_4^2 O_4^2 + B_4^4 O_4^4 + B_6^0 O_6^0 + B_6^2 O_6^2 + B_6^4 O_6^4 + B_6^6 O_6^6. \tag{5}$$

However, we used the conventional zero-field splitting Hamiltonian, which is still widely used (Bleaney and Stevens 1953, Abragam and Bleaney 1970, Pool and Farach 1972):

$$\begin{aligned} H_{zfs} = {} & D[S_z^2 - S(S+1)/3] + E(S_+^2 + S_-^2)/2 + F[35S_z^4 - 30S(S+1)S_z^2 + 25S_z^2 \\ & - 6S(S+1) + 3S^2(S+1)^2]/180 + B_4^2 O_4^2 \\ = {} & B_2^0 O_2^0 + B_2^2 O_2^2 + B_4^0 O_4^0 + B_4^2 O_4^2 \end{aligned} \tag{6}$$

where D and E are the second-order axial and the rhombic zero-field splitting parameters, respectively, and F is a fourth-order one. The relationship between the notations are $D = 3B_2^0$, $E = 3B_2^2$ and $F = 180B_4^0$ (Abragam and Bleaney 1970). Here, we used only four parameters instead of the nine in equation (5) because these parameters turned out to be sufficient to fit our experimental data. The hyperfine interaction is

$$H_h = \boldsymbol{S} \cdot \mathbf{A} \cdot \boldsymbol{I} \tag{7}$$

where $\mathbf{A}$ represents the hyperfine tensor, and $\boldsymbol{I}$ is the nuclear spin vector.

The maximum separation of the resonance fields due to the D-tensor was observed when the magnetic field was applied along the $\bar{a} + 45°$ (i.e. $c + 135°$) direction in the ca-plane of the crystal, and this direction was designated as the z axis of the D-tensor. We carried out a coordinate transformation from the principal axes of the D-tensor to the crystallographic axes in order to analyse the experimental data obtained on the crystallographic principal planes. The energy levels due to equations (2) and (6) were obtained by numerically diagonalizing the 6×6 matrix of the $|S, S_z\rangle$ states with $S = \frac{5}{2}$ by employing the Jacobi rotation method. In order to obtain the EPR parameters from the measured spectra, all allowed transitions corresponding to the resonance lines were considered. These transitions between energy level ($|S_z\rangle$ only) pairs are indicated for each curve in figures 3, 4 and 5. The EPR parameters were determined by a least-square fit to the experimental data, and we selected the parameters which best satisfy simultaneously the resonance fields measured on the crystallographic ab-, bc- and ca-planes.

Since the hyperfine interaction turns out to be much smaller than the Zeeman and crystal field interactions, it is sufficient to regard it as the first-order perturbation of equations (2) and (6). The EPR parameters which we obtained for Mn^{2+} in ferroelastic $BiVO_4$ are summarized in table 1 along with those previously reported by Baran *et al* (1985).

The intensity of the EPR spectra is found to decrease as the temperature increases. The thirty EPR lines degenerated into six lines of the transition $M = \frac{1}{2} \leftrightarrow -\frac{1}{2}$ when the rotation pattern of the resonance fields in the para-elastic phase was obtained. The EPR parameters in the para-elastic phase are summarized in table 2 along with those previously reported by Baran *et al* (1985).

6. Results and discussion

The principal x, y and z axes of the D-tensor of the Mn^{2+} ion in the ferroelastic phase of $BiVO_4$ single crystal are found to lie along the crystallographic $\bar{b}$, $c+45°$ (i.e. $\bar{a} - 45°$) and $\bar{a} + 45°$ (i.e. $c + 135°$) axes, respectively. This designation is, as shown in figure 7, different from that of Mn_I reported by Baran *et al*. Their assignment of the principal axes appears to be incorrect by 45°, as can be seen in table 1. Their improper designation of the principal axes may be reflected by the largest value of b_2^{-2} compared with $b_2^0(D)$ and $b_2^2(E)$. If the axes system of Mn_I centre is transformed to that of ours shown in figure 7, the Mn_I centre could be better represented by the parameters of the present work.

There is some confusion concerning the negative components in equation (3) with $q < 0$ and the explicit transformation relationships (Rudowicz 1987). Most books on EPR (e.g. Abragam and Bleaney 1970) have ignored these parameters. Baran *et al*

Table 1. Comparison of EPR parameters for Mn^{2+} in ferroelastic $BiVO_4$ at room temperature†.

	Impurity	g	D/h	E/h	F/h	b_4^2/h	b_4^4/h	b_2^{-2}/h	b_4^{-2}/h	b_4^{-4}/h	A/h	Principal axes[a]
Present work	Mn	1.9940	2.443	0.4912	0.094	0.0	—	—	—	—	$A_x = 0.27 \pm 0.02$	$x = \bar{b}$
		±0.0009	±0.002	±0.0009	±0.002	—	—	—	—	—	$A_y = 0.25 \pm 0.02$	$y = c + 45°$
		—	—	—	—	—	—	—	—	—	$A_z = 0.33 \pm 0.02$	$z = \bar{a} + 45°$
Baran *et al* [b] (1985)	Mn_I	1.994	0.492	0.04	0.02	0.18	0.03	4.38	0.02	0.006	0.279	$x = a$, $y = \bar{c}$
		±0.001	±0.006	±0.02	±0.03	±0.05	±0.03	±0.02	±0.06	±0.05	±0.006	$z = b$
	Mn_{II}	1.994	3.12	1.41	—	$b_4^m/h < 0.09$					0.25	[c]
		±0.002	±0.09	±0.09	—						±0.02	—

† The units are all in GHz except for the g-value.

[a] The relationship between the crystallographic axes and the principal axes of the D-tensor.

[b] The units and notation have been converted for comparison with our data.

[c] $|za| = |z\bar{c}| = |zb| = 0.58 \pm 0.03$, $|xa| = 0.71 \pm 0.03$.

Table 2. A comparison of EPR parameters of Mn^{2+} in para-elastic $BiVO_4$†.

	g	D/h	E/h	F/h	A/h	b_4^4
Present work	1.994	0.000	0.000	0.00	0.25	
$T = 535$ K	±0.001	±0.004	±0.004	±0.01	±0.01	
Mn_I[a]	1.994	≈0		0.14		0.009
$T = 650$ K				±0.05		±0.003

† The units are all in GHz except for the g-value.
[a] The units and notations of Baran *et al* (1985) have been converted for comparison with our data.

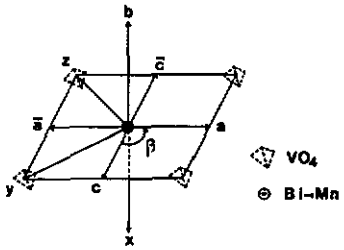

Figure 7. The relationship between the principal axes of the D-tensor of Mn^{2+} and the crystallographic axes on the (020)-plane of figure 1 in the ferroelastic phase.

(1985) obtained parameters with higher-order components and negative q as shown in table 1. However, although we adopted conventional zero-field splitting parameters without negative components, our calculated angular dependences for the resonance fields, drawn with full curves, are in good agreement with the experimental results as shown in figures 3, 4 and 5. This shows that our parameters, without negative and higher-order terms, are good enough to explain the experimental data. Our crystal is the same one used by Choh *et al* (1985) and Lim *et al* (1989) to report on ^{51}V NMR in $BiVO_4$. The weak signal with the six-line hyperfine structure to the left of signal 1 in figure 2 is found to be a forbidden transition between $|\frac{1}{2}\rangle$ and $|\frac{5}{2}\rangle$. The points of the forbidden transition are indicated by full circles in figure 5 and the broken curve is the result of our calculations. There is no indication of any other Mn^{2+} centres, such as Mn_{II} (Baran *et al* 1985), which has a vacancy in the immediate environment and different principal axes, in our crystal, possibly due to the extremely low Mn^{2+} concentration.

As can be seen in table 2, the zero-field splitting parameters of Mn^{2+} centre are zero in the para-elastic phase. While the central transition stays constant as displayed in figure 6, implying that the g-value is temperature independent, the D and E are, however, found to decrease as the temperature increases. The result of plotting the zero-field splitting parameters against temperature is shown in figure 8, where the parameters go to zero almost continuously as the temperature approaches T_c. Since D and E are found to be zero above T_c, the phase transition temperature in $BiVO_4$ can be accurately determined by the EPR technique. The sample, which had a single domain, preserved its domain state after the temperature was raised above T_c and then cooled down to room temperature. The D-value of our Mn^{2+} centre decreases

as the temperature increases as with the Mn_I centre (Baran *et al* 1986). However, we found inconsistencies in their D-values: for example, $D = 0.492$ GHz (Baran *et al* 1985) and 1.95 GHz (Baran *et al* 1986) at room temperature.

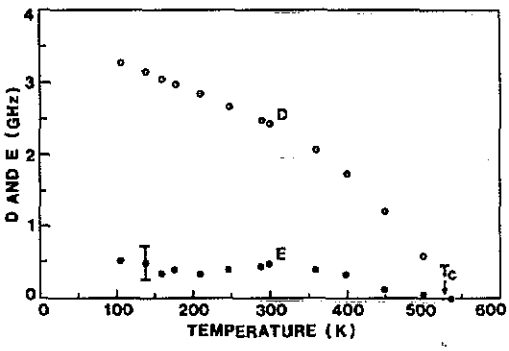

Figure 8. Temperature dependence of D and E for the Mn^{2+} in the $BiVO_4$ single crystal. The error range of D-value is within the open circles at given temperatures. However, the error bar of E is large because E itself is very small.

Several possibilities are examined for the Mn^{2+} centre in the $BiVO_4$ crystal. First, if the Mn^{2+} resides in a structural vacancy, such as the geometric centres of the (040)- and $(0\frac{4}{3}0)$-planes in figure 1, the principal axis of the D-tensor in the ca-plane should be parallel to the a or the c axes. However, since the results in figure 5 deviate from the a and c axes, this first possibility is ruled out. Next, one may propose that the Mn^{2+} ion can occupy either the Bi^{3+} or V^{5+} ion site because the y and z axes of the D-tensor are nearly parallel to the direction joining V to Bi (or Bi to V) in the ca-plane. Meanwhile, the principal axes of the electric field gradient (EFG) tensor of the ^{51}V nucleus are known to lie along the crystallographic axes (Choh *et al* 1985). Moreover, we compared the temperature dependence of the D-value of the Mn^{2+} ion with that of e^2qQ/h of ^{51}V in $BiVO_4$. The variation in the D-value with temperature is considered to be related to the displacement of the Mn^{2+} ion. Since the D-value of Mn^{2+} is dependent on temperature in the present work, the internal crystal field at the lattice site occupied by the impurity is definitely changing with temperature. According to the literature D and e^2qQ/h can be related (Burns 1962). There is also a similarity between D and e^2qQ/h in the EPR and NMR Hamiltonians (Choh *et al* 1989). Since the e^2qQ/h of ^{51}V in $BiVO_4$ is nearly independent of the temperature (Lim *et al* 1989), it is reasonable to argue that the Mn^{2+} ion in the $BiVO_4$ crystal does not occupy the V site. Accordingly, the second possibility of substituting for the V atom is also eliminated.

The remaining one, substitution for Bi^{3+}, seems more reasonable because the principal axes of the D-tensor of the Mn^{2+} centre are closely associated with the crystallographic axes. As shown in figure 7, the z axis of the D-tensor is along the direction of the shorter Bi–VO_4 bond (7.2514 Å) and the y axis is along the longer one (7.3000 Å). Because the displacement of the Bi^{3+} ions plays a major role in the phase transition (Wood and Glazer 1980), the substitution of Bi by Mn^{2+} is consistent with our results of the temperature dependence of the D-value of Mn^{2+} in $BiVO_4$. As far as the ionic charge state is concerned, Mn^{2+} is closer to Bi^{3+} than to V^{5+}.

Considering all these possibilities, we propose that the Mn^{2+} ion replaces the Bi^{3+} ion without nearby charge compensation. This proposal is consistent with that made by Baran *et al* (1985).

7. Summary

The EPR parameters and the principal axes of the D-tensor of the Mn^{2+} centre in the ferroelastic phase of $BiVO_4$ have been determined in terms of the spin Hamiltonian: $H = \beta(\boldsymbol{B}\cdot\mathbf{g}\cdot\boldsymbol{S}) + D[S_z^2 - S(S+1)/3] + E(S_+^2 + S_-^2)/2 + F[35S_z^4 - 30S(S+1)S_z^2 + 25S_z^2 - 6S(S+1) + 3S^2(S+1)^2]/180 + B_4^2O_4^2 + \boldsymbol{S}\cdot\mathbf{A}\cdot\boldsymbol{I}$ with parameters $g = 1.9940 \pm 0.0009$, $D/h = 2.443 \pm 0.002$, $E/h = 0.4912 \pm 0.0009$, $F/h = 0.094 \pm 0.002$, $B_4^2/h = 0.0$, $A_x/h = 0.27 \pm 0.02$, $A_y/h = 0.25 \pm 0.02$, and $A_z/h = 0.33 \pm 0.02$ GHz; and $x = \bar{b}$, $y = c + 45°$, and $z = \bar{a} + 45°$ at room temperature. The EPR parameters in the para-elastic phase have also been determined: $g = 1.994 \pm 0.001$, $D/h = 0.000 \pm 0.004$, $E/h = 0.000 \pm 0.004$, $F/h = 0.00 \pm 0.01$, $A/h = 0.25 \pm 0.01$ GHz at 535 K. The experimental data can be explained satisfactorily with only four parameters instead of the nine claimed for the orthorhombic system. The temperature dependence of the EPR parameters for the Mn^{2+} impurity in the range 107–535 K is examined and the D- and E-values are found to decrease as the temperature increases and go to zero as $T \leqslant T_c$. It is proposed that the Mn^{2+} ion substitutes for the Bi^{3+} ion without nearby charge compensation. This Mn^{2+} centre in $BiVO_4$ has the correct principal axes system of the D-tensor compared with the previously reported Mn_I centre.

Acknowledgments

We gratefully acknowledge the financial support of the Basic Science Research Institute Programme of the Ministry of Education (1989–94) and access to the EPR spectrometer, with the helpful assistance of Mr K J Song at the Korea Basic Science Centre. One of the authors (THY) is grateful to the KOSEF for a fellowship during the preparation of his doctoral dissertation (1990–91). This work was also supported in part by KOSEF through the SRC of Excellence Programme (1991–94).

References

Abragam A and Bleaney B 1970 *Electron Paramagnetic Resonance of Transition Ions* (Oxford: Oxford University Press) ch 3 and ch 7

Altshuler S and Kozyrev B M 1974 *Electron Paramagnetic Resonance in Compounds of Transition Elements* (New York: Wiley) ch 3

Baran N P, Barchuk V I, Grachev V G and Krulikovskii B K 1985 *Sov. Phys.-Crystallogr.* **30** 410

—— 1986 *Sov. Phys.-Solid State* **28** 485

Bierlein J D and Sleight A W 1975 *Solid State Commun.* **16** 69

Bleaney B, Scovil H E D and Trenam R S 1954 *Proc. R. Soc.* A **223** 15

Bleaney B and Stevens K W H 1953 *Rep. Prog. Phys.* **16** 108

Burns G 1962 *Phys. Rev.* **123** 1634

Choh S H, Kim H T, Choh H K, Han C S, Choi D and Kim J N 1989 *Bull. Mag. Res.* **11** 371

Choh S H, Moon E Y, Park Y H and Jang M S 1985 *Japan. J. Appl. Phys.* **24** 640

David W I F, Glazer A M and Hewat A W 1979 *Phase Trans.* **1** 155

Dudnik E P, Gene B B and Menushkina I E 1979 *Izv. Akad. Nauk* **43** 1723

Lim A R, Choh S H and Jang M S 1989 *Ferroelectrics* **94** 389

Moon E Y, Choh S H, Park Y H, Yeom H Y and Jang M S 1987 *J. Phys. C: Solid State Phys.* **20** 1867

Newman D J and Urban W 1975 *Adv. Phys.* **24** 793

Pinczuk A, Burns G and Dacol F H 1977 *Solid State Commun.* **24** 163

Pinczuk A, Welter B and Dacol F H 1979 *Solid State Commun.* **29** 515

Pool C P, Jr and Farach H A 1972 *The Theory of Magnetic Resonance* (New York: Wiley) ch 1 and ch 12
Roth R S and Waring J L 1963 *Am. Mineral.* **48** 1348
Rudowicz C 1985 *J. Phys. C: Solid State Phys.* **18** 1415
—— 1986 *J. Chem. Phys.* **86** 5045
—— 1987 *Mag. Res. Rev.* **13** 1
Sleight A W, Chen H Y, Ferretti A and Cox D E 1979 *Mater. Res. Bull.* **14** 1571
Wood I G and Glazer A M 1980 *J. Appl. Crystallogr.* **13** 217
Yeom T H, Choh S H and Jang M S 1990 *Bull. Korean Phys. Soc.* **8** 277